Chirality and Bianisotropy Effects in Plasmonic Metasurfaces and Their Application to Realize Ultrathin Optical Circular Polarizers

***Andrea Alù*[1], *Yang Zhao*[1], *and Xing-Xiang Liu*[1]**

[1]Department of Electrical Engineering, University of Texas at Austin, 1 University Station, Austin, TX 78712, USA
Corresponding author email: alu@mail.utexas.edu

Abstract

In this paper we develop a rigorous analytical theory relating the effective impedance of plasmonic metasurfaces to a generalized form of polarizability, which compactly describes the electric, magnetic and magneto-electric response of the individual inclusions and the overall array coupling. We apply this theory to the design of plasmonic metasurfaces composed of lithographically printed planar inclusions, showing that their inherent chiral and bianisotropic response may be exploited to produce ultrathin optical circular polarizers. Bianistropic effects, particularly relevant to enhance the response to circularly polarized light, may be maximized in specific incidence planes, as a function of the inclusion symmetries.

1. Introduction

Generation and detection of circular polarization of light is essential to a variety of fields including optical communication, optical data storage, sensing, imaging and display technologies. Since circular polarization is based on phase shifts between two perpendicular components of electric fields, it is inherently difficult to be achieved within a distance shorter than one quarter wavelength. The recent development of ultrathin plasmonic metasurfaces may pave the way to the realization of quarter-wave plates with only few nanometer thickness, as we discuss in the following. Metasurfaces [1-3] are the two dimensional version of metamaterials, which consist of artificial subwavelength inclusions engineered to achieve anomalous electromagnetic properties beyond what is naturally available from their constituent materials. Optical metamaterials base their exotic properties on resonant inclusions, in particular on the plasmonic effects of small nanoparticles with specific geometry. Similarly, a planar array of resonant inclusions may realize an averaged surface impedance (or admittance) [4] with exotic values. This is similar to the concepts introduced several years ago to simplify the design and modeling of frequency selective surfaces at microwave frequencies [5]. Extended to optics, the optical surface impedance of these planar arrays can compactly characterize their anomalous light interaction. In this work, we aim at modeling thin plasmonic metasurfaces with a surface admittance tensor based on the dipolar polarizability of the inclusions forming the array, rigorously taking into account the full dynamic interaction within the array and the possible cross-polarization coupling in different configurations. We apply these concepts to show both theoretically and numerically that it may be possible to realize individual ultrathin plasmonic metasurfaces to generate and filter circular polarization, despite their ultrathin geometries.

2. Theoretical Analysis

Consider an optically thin metasurface located in the $z=0$ plane, formed by arbitrarily shaped plasmonic nanoparticles embedded in a rectangular lattice with periods d_x and d_y. In the following analysis, we assume that the lattice constants are much smaller than the wavelength of operation and that the inclusions are not too densely packed, so that the optical wave interaction can be modeled using the dipolar approximation with good accuracy. We further assume that the inclusions are sufficiently thin in the z direction to ensure that only an optical displacement current tangential to the surface may be induced. When excited by an external plane wave with arbitrary polarization and incidence angle θ, the inclusions may support an electric dipole moment parallel to the surface and a magnetic dipole moment normal to it, which may be related to the local electric and magnetic fields (defined as the fields on the inclusion location when absent) through the generalized polarizability tensor:

$$\begin{pmatrix} \mathbf{p}/\varepsilon_0 \\ \eta_0 m/\mu_0 \end{pmatrix} = \begin{pmatrix} \underline{\boldsymbol{\alpha}}_{ee} & \boldsymbol{\alpha}_{em} \\ -\boldsymbol{\alpha}_{em}^T & \alpha_{mm} \end{pmatrix} \cdot \begin{pmatrix} \mathbf{E}_{loc} \times \hat{\mathbf{z}} \\ \eta_0 \mathbf{H}_{loc} \cdot \hat{\mathbf{z}} \end{pmatrix}, \tag{1}$$

978-1-4244-6051-9/11/$26.00 ©2011 IEEE

where $\eta_0, \varepsilon_0, \mu_0$ are the background characteristic impedance, permittivity and permeability respectively, $\underline{\underline{\boldsymbol{\alpha}}}_{ee}$ is the electric transverse polarizability tensor, which is symmetric due to reciprocity under the assumption that all inclusions are made of reciprocal materials; α_{mm} is the magnetic polarizability response, which is a scalar for an ultrathin surface; and $\boldsymbol{\alpha}_{em}$ takes into account of possible bianisotropic effects at the inclusion level. These quantities compactly describe the electric and magnetic response of the isolated inclusion within the dipolar limit.

In a planar array, the local fields on the inclusion are the superposition of the impinging fields and the radiation coupling due to the presence of all the other inclusions in the array. Therefore, the metasurface polarization may be compactly described through a generalized array polarizability tensor $\underline{\underline{\boldsymbol{\alpha}}}_s$ which includes the full dynamic coupling among the inclusions through the interaction dyadics $\mathbf{C}$ [6-12]:

$$\begin{pmatrix} \mathbf{p}/\varepsilon_0 \\ \eta_0 m/\mu_0 \end{pmatrix} = \left(\begin{pmatrix} \underline{\underline{\boldsymbol{\alpha}}}_{ee} & \boldsymbol{\alpha}_{em} \\ -\boldsymbol{\alpha}_{em}^T & \alpha_{mm} \end{pmatrix}^{-1} - \begin{pmatrix} \underline{\underline{\mathbf{C}}}_{tt} & \mathbf{C}_{tz} \\ -\mathbf{C}_{tz}^T & C_{zz} \end{pmatrix} \right)^{-1} \cdot \begin{pmatrix} \mathbf{E}_{inc} \times \hat{\mathbf{z}} \\ \eta_0 \mathbf{H}_{inc} \cdot \hat{\mathbf{z}} \end{pmatrix} = \underline{\underline{\boldsymbol{\alpha}}}_s \cdot \begin{pmatrix} \mathbf{E}_{inc} \times \hat{\mathbf{z}} \\ \eta_0 \mathbf{H}_{inc} \cdot \hat{\mathbf{z}} \end{pmatrix}, \tag{2}$$

where $\underline{\underline{\boldsymbol{\alpha}}}_s = \begin{pmatrix} \alpha_{xx}^{ee} & \alpha_{xy}^{ee} & \alpha_{xz}^{em} \\ \alpha_{yx}^{ee} & \alpha_{yy}^{ee} & \alpha_{yz}^{em} \\ \alpha_{zx}^{me} & \alpha_{zy}^{me} & \alpha_{zz}^{mm} \end{pmatrix} = \begin{pmatrix} \underline{\underline{\boldsymbol{\alpha}}}_s^{ee} & \boldsymbol{\alpha}_s^{em} \\ \left(-\boldsymbol{\alpha}_s^{em}\right)^T & \alpha_s^{mm} \end{pmatrix}$. In general, its elements are dependent on the incidence angle, as a symptom of spatial dispersion in the array, due to the influence of the coupling dyadics. For small periods, the spatial dispersion effects are however negligible and Eq. (2) may compactly describe the array interaction for arbitrary excitation.

In particular, for transverse electric (TE) excitation, the reflection and transmission coefficients may be related to the general polarizability tensor elements as

$$\begin{aligned} T_{ee} &= 1 - jk_0 \left(\frac{sec\theta \alpha_{yy}^{ee} + sin\theta tan\theta \alpha_{zz}^{mm}}{2 d_x d_y} \right), \quad T_{me} = -jk_0 \frac{\alpha_{xy}^{ee} + sin\theta \alpha_{xz}^{em}}{2 d_x d_y} \\ R_{ee} &= -jk_0 \left(\frac{sec\theta \alpha_{yy}^{ee} + sin\theta tan\theta \alpha_{zz}^{mm}}{2 d_x d_y} \right), \quad R_{me} = -jk_0 \frac{\alpha_{xy}^{ee} + sin\theta \alpha_{xz}^{em}}{2 d_x d_y} \end{aligned}, \tag{3}$$

whereas for transverse magnetic (TM) excitation:

$$\begin{aligned} T_{em} &= -jk_0 \frac{\alpha_{xy}^{ee} - sin\theta \alpha_{xz}^{em}}{2 d_x d_y}, \quad T_{mm} = 1 - jk_0 \frac{cos\theta \alpha_{xx}^{ee}}{2 d_x d_y} \\ R_{em} &= -jk_0 \frac{\alpha_{xy}^{ee} - sin\theta \alpha_{xz}^{em}}{2 d_x d_y}, \quad R_{mm} = -jk_0 \frac{cos\theta \alpha_{xx}^{ee}}{2 d_x d_y} \end{aligned}, \tag{4}$$

where k_0 is the propagation constant in the background medium.

After some mathematical manipulations, it may be shown that the difference between the transmission coefficients for the two circular polarizations is given by the simple formula:

$$\Delta = T_{LL} - T_{RR} = \frac{k_0 \alpha_{xz}^{em} sin\theta}{d_x d_y}, \tag{5}$$

provided that $y = 0$ is the incidence plane. In this formula, T_{LL} (T_{RR}) is the transmission coefficient of left- (right-) handed circular polarization for same excitation. It is evident from Eq. (5) that a single ultrathin metasurface may differentiate circular polarization under two necessary conditions: (a) the angle of incidence should be oblique; (2) the electromagnetic polarizability α_{xz}^{em} is nonzero. This is a very general result, independent on the specific metasurface geometry or constituent material, under the only assumptions that the metasurface is made of reciprocal materials and its thickness is negligible compared to the wavelength of operation, i.e. Eq. (1) applies. Indeed, it has been extensively

discussed experimentally [13] that a 'chiral' metasurface may produce large extinction ratios between left hand (LCP) and right hand circular polarizations (RCP) at oblique incidence. Eq. (5) compactly describes this property and ensures that the possibility to distinguish circular polarizations depends on the inclusion symmetry, since a nonzero α_{xz}^{em} requires no mirror symmetry along the axis orthogonal to the plane of incidence.

Although at normal incidence LCP and RCP are indistinguishable, i.e., $|T_{LL}| = |T_{RR}|$, it may be possible to generate circular polarizations with linear inputs through an ultrathin metasurface when the inclusions are tailored to create transmission coefficients equal to the classical Jone's matrix of a quarter wave plate. The surface admittance tensor of such ultrathin quarter-wave plate should be $\underline{\boldsymbol{\alpha}}_s^{ee} = \frac{\sqrt{2} d_x d_y}{\omega \sqrt{\mu_0 \epsilon_0}} \begin{pmatrix} -\exp(-i\pi/4) & 0 \\ 0 & \exp(+i\pi/4) \end{pmatrix}$. We verify both these possibilities to realize circular polarizers with a single ultrathin optical surface in the following section.

3. Numerical Simulations

Rigorous full wave numerical simulations have been conducted to demonstrate the functionality of the proposed geometries in practical setups using commercially available software based on finite integration techniques [14]. Figure 1 shows the transmission coefficients and degree of linear polarization of a single plasmonic metasurface consisting of interleaved silver nanorods aligned in an orthogonal fashion, whose permittivity is modeled using the Drude permittivity model [15]. The unit cell is rectangular, with periods $d_x = 122nm$ and $d_y = 98nm$, the horizontal and vertical nanorods have a length of 62nm and 78nm, respectively, with same width 20nm and thickness 28nm. This design validates the idea that using ultrathin plasmonic metasurfaces may realize few nanometer thick quarter-wave plates at normal incidence by designing both sets of nanorods to operate slightly off resonance such that the transmission through the metasurface adds a phase difference of 90° for one linear polarization with respect to the other at the resonant wavelength of 600nm. Figure 1(b) proves that such metasurface may provide large degree of polarization over a broad frequency range, spanning from visible to near-IR regime, providing unique potentials for circular polarization generation. Figure 2 confirms the possibility of distinguishing LCP and RCP under oblique incidence using U-shaped inclusions, as indicated in the insets. When we excite the metasurface at 45° in the plane of symmetry of the inclusion [Figure 2(b)], strong asymmetry between T_{LL} and T_{RR} are observed, due to the lack of mirror symmetry in the x direction; on the contrary, for either normal incidence or oblique incidence in the plane of symmetry [Figure 2(a)], the two circular polarizations are indistinguishable according to (5), as verified in panel (a).

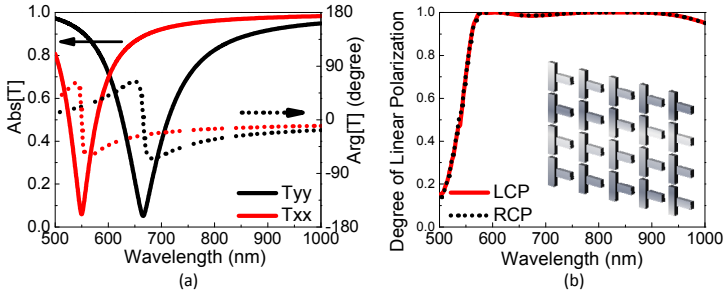

Figure 1. a) Amplitude and phase of transmission coefficient for an individual metasurface with T shaped inclusions at normal incidence. b) Degree of linear polarization for T shaped inclusion (geometry in the inset).

4. Conclusions

We have shown here that a properly designed plasmonic metasurface may realize an ultrathin circular polarization filter in different configurations and forms of excitation. We have theoretically proposed and numerically verified the design of an ultrathin plasmonic quarter-wave plate for excitation at normal incidence and of a magneto-electric metasurface operating as a circular polarizer for oblique incidence excitation. Our results may pave the way to the practical manipulation and control of light polarization for a variety of applications. They may also introduce novel concepts in the realization and understanding of plasmonic metasurfaces and metamaterials. This work has been partially supported by NSF with a CAREER award number ECCS-0953311 and an ONR MURI award number N00014-10-1-0942.

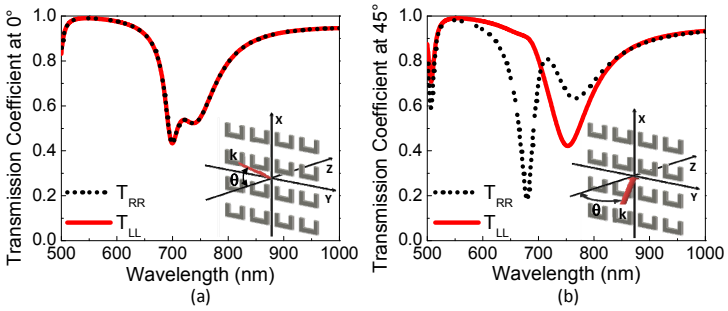

Figure 2. a) Plasmonic metasurface with U-shaped inclusions and mirror symmetry in the *y* direction presents indistinguishable T_{LL} and T_{RR} at oblique incidence in the plane y=0. b) The separation of T_{LL} and T_{RR} for oblique incidence is verified, as predicted by Eq. (5), within the x=0 incidenceplane.

5. References

1. E. F. Kuester, M. A. Mohamed and C. L. Holloway, "Averaged transition conditions for electromagnetic field at a metafilm," *IEEE Trans. Antenn. Propag*., **51**, 2003, pp. 2641–2651.

2. H. Mosallaei and K. Sarabandi, "A one-layer ultra-thin meta-surface absorber," Proc. of AP-S, Washington, DC, 2005.

3. C. L. Holloway, M. A. Mohamed and E. F. Kuester, "Reflection and transmission properties of a metafilm: with an application to a controllable surface composed of resonant particles," *IEEE Trans. Electromagn. Compat.,* **47**, 2005, pp. 853-865.

4. A. Alù and N. Engheta, "Three-dimensional nanotransmission lines at optical frequencies: A recipe for broadband negative-refraction optical metamaterials," *Phys. Rev. B*, **75**, pp. 024304, 2007.

5. B. A. Munk, *Frequency Selective Surfaces: Theory and Design*, *First Edition*, New York, Wiley, 2000.

6. R. A. Shore, and A. D. Yaghjian, "Travelling electromagnetic waves on linear periodic arrays of lossless spheres," *Electronics Letters*, **41**, 2005, pp. 578-579.

7. A. Alù, and N. Engheta, "Theory of linear chains of metamaterial/plasmonic particles as sub-diffraction optical nanotransmission lines," *Phys. Rev. B*, **74**, 2006, 205436.

8. F. J. Garcia de Abajo, "Light scattering by particle and hole arrays," *Rev. Mod. Phys.,* **79**, 2007, pp. 1267-1290.

9. A. J. Viitanen, I. Hanninen, and S. A. Tretyakov, "Analytical model for regular dense arrays of planar dipole scatterers," *Progress in Electromagnetics Research*, **38**, 2002, pp. 97-110.

10. M. Englund, and A. J. Viitanen, "A planar dipole array formed by small resonant particles," *Microw. Optical Technology Letters*, **49**, 2007, pp. 2419-2422.

11. P. Belov and C. Simovski, "Homogenization of electromagnetic crystals formed by uniaxial resonant scatterers," *Phys. Rev. E*, **72**, 2005, 026615.

12. A. Alù and N. Engheta, "Optical Wave Interaction with Two-Dimensional Arrays of Plasmonic Nanoparticles," in Structured Surfaces as Optical Metamaterials, Cambridge University Press, in press.

13. E. Plum, X.-X. Liu, V.A. Fedotov, Y. Chen, D.P. Tsai and N. I. Zheludev, "Metamaterials: optical activity without chirality," *Phys. Rev. Lett.*, **102**, 2009, pp. 113902.

14. CST Microwave Studio™ 2010, CST of America, Inc.

15. P. B. Johnson and R. W. Christy, "Optical constants of the noble metals," *Phys. Rev. B*, **6**, 1972, pp. 4370-4379.